ACS SENSORS

pubs.acs.org/acssensors

Article

Effect of Serum on Electrochemical Detection of Bioassays Having Ag Nanoparticle Labels

Nicole E. Pollok,[§] Yi Peng,[§] Charlie Rabin, Ian Richards, and Richard M. Crooks*

Cite This: *ACS Sens.* 2021, 6, 1956–1962

Read Online

ACCESS | Metrics & More | Article Recommendations | Supporting Information

ABSTRACT: The effect of serum on electrochemical detection of bioassays having silver nanoparticle (AgNP) detection labels was investigated. Both a model assay and an antigen-specific sandwich bioassay for the heart failure marker NT-proBNP were examined. In both cases, the AgNP labels were conjugated to a detection antibody. Electrochemical detection was carried out using a galvanic exchange/anodic stripping voltammetry method in which Au^{3+} exchanges with AgNP labels. The assays were carried out using a paper-based electrode platform. The bioassays were exposed to different serum conditions prior to and during detection. There are three important outcomes reported in this article. First, both the model- and antigen-specific assays could be formed in undiluted serum with no detectable interferences from the serum components. Second, to achieve the maximum possible electrochemical signal, the highest percentage of serum that can remain in an assay buffer during electrochemical detection is 0.25% when no washing is performed. The assay results are rendered inaccurate when 0.50% or more of serum is present. Third, the factors inhibiting galvanic exchange in serum probably relate to surface adsorption of biomolecules onto the AgNP labels, chelation of Au^{3+} by serum components, or both. The results reported here provide general guidance for using metal NP labels for electrochemical assays in biofluids.

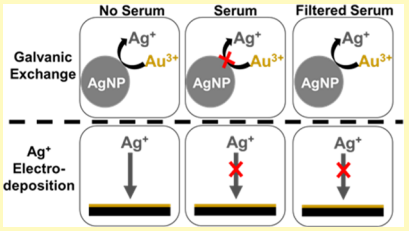

KEYWORDS: *serum, silver nanoparticles, metalloimmunoassay, electrochemical label, galvanic exchange, anodic stripping voltammetry*

There are three key steps to executing a typical bioassay: capture of the analyte of interest, removal (washing) of excess reagents, and detection. At each of these steps, the detection medium can either play an advantageous[1,2] or a detrimental[3] role. In the present study, we evaluated the effect of serum on a previously reported method for detecting silver nanoparticle (AgNP) labels that combines galvanic exchange (GE) and anodic stripping voltammetry (ASV). Scheme 1 illustrates the GE/ASV method. In the first step (Scheme 1a), Au predeposited onto the working electrode (WE) is oxidized and then the resulting electrogenerated Au^{3+} oxidizes AgNPs in the vicinity of the electrode surface. During the second step (Scheme 1b), the resulting Ag^+ is concentrated onto the electrode surface by electrodeposition and then detected by ASV. Though we examined the effect of serum on this GE/ASV detection method, the results are generally applicable to many different types of electrochemical bioassays.

Electrochemical biosensors are powerful tools used to monitor medical conditions at home,[4,5] in clinics,[6−8] and in hospitals.[9,10] Human biomarkers for point-of-care and point-of-need sensors are found in matrixes including sweat,[11,12] saliva,[13−15] and whole blood[16,17] (among others).[18] Serum is another common matrix used for bioassays. It is the fluid and solute component of whole blood that does not play a role in clotting. It includes all proteins not used in clotting, all electrolytes, antibodies (Abs), antigens, hormones, and exogenous substances.[19,20] Human serum albumin is the most abundant protein in human blood plasma, and it constitutes about 50% of the proteins in serum.[19] Due to the

Scheme 1. Illustration of the GE/ASV Detection Method[a]

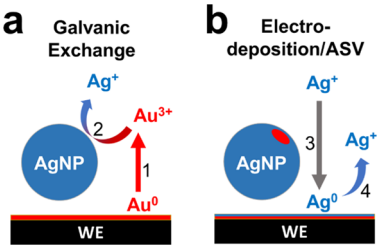

[a]Electrochemical procedures: in step 1, the potential of the WE is stepped from 0 to 0.80 V for 12.0 s to electro-oxidize zerovalent Au (present on the WE surface) to Au^{3+}. This initiates GE (step 2). In step 3, the WE potential is stepped from 0 to −0.70 V for 50 s to electrodeposit the resulting Ag^+ onto the WE as zerovalent Ag. Finally, in step 4, ASV is used to oxidize Ag, present on the WE, by sweeping the WE potential from −0.70 to 0.20 V at 50.0 mV/s. Prior studies have shown that the electrochemical signal is maximized by carrying out step 4 twice and using the charge under the second ASV peak to determine the amount of AgNP labels present.

Received: March 2, 2021
Accepted: April 8, 2021
Published: April 22, 2021

https://doi.org/10.1021/acssensors.1c00446
ACS Sens. 2021, 6, 1956–1962

relatively high abundance of albumin in serum, its electrochemistry has been studied. For example, both the oxidized and reduced forms of bovine serum albumin (BSA) exhibit reversible electron transfer when strongly adsorbed to a hanging mercury drop electrode through the interaction of exposed disulfide bonds with the mercury surface.[3]

Signal amplification is often a key component of bioassays. Amplification is usually accomplished using enzyme labels; for example, in enzyme-linked immunosorbent assays.[21,22] Over the past 20 years, however, there has been growing interest in using metallic or semiconducting nanoparticles (NPs) for signal amplification due to their generally higher stability, lower cost, and faster read-out times.[23,24] More specifically, AgNPs and gold NPs (AuNPs) conjugated to recognition elements, such as Abs,[25−30] nucleic acids,[31−33] or aptamers,[34] are becoming increasingly common. To ensure the stability of the metal label in complex media, many protocols include surface-modification steps; for example, addition of thiolated polyethylene glycol.[35] Furthermore, although a relatively complex matrix, serum can also work as an effective NP stabilizing agent and a conductive medium for electrochemical analysis.[1,36−38] In fact, in 2009, Murawala et al. described a simple and convenient one-step, room-temperature method for the synthesis of BSA-capped AgNPs and AuNPs. The resulting NPs were easily dispersible in water and could withstand dynamic salt conditions, all of which are important characteristics of NPs used in bioassays.[38]

A previous work from our group has shown that metalloimmunoassays can be formed in undiluted human serum,[25] but that the GE/ASV detection process is inhibited. In the present article, we aim to elucidate the factors leading to inhibition. Specifically, we will show that (1) both a model and an antigen-specific metalloimmunoassay can be formed in serum; (2) systematic analysis of washing steps reveals the maximum amount of serum that can remain during detection to yield full recovery of the Ag signal; and (3) there are differences in detectability when serum or filtered serum is used. These findings should be of broad interest to those interested in carrying out electrochemical bioassays on analytes found in serum.

EXPERIMENTAL SECTION

Chemicals and Materials. NaCl, NaOH, HCl, KNO_3, $NaIO_4$, Whatman grade 1 chromatography paper (180 μm thick, 20 cm × 20 cm sheets, linear flow rate of water = 0.43 cm/min), and siliconized low-retention microcentrifuge tubes were purchased from Fisher Scientific (Pittsburgh, PA). $HAuCl_4$, $AgNO_3$, phosphate-buffered saline (PBS, pH = 7.4, P3813), superblock blocking buffer containing PBS (SBB) (cat. no. 37515), polyoxyethylene (20) sorbitan monolaurate (Tween-20), 4-(2-hydroxyethyl)-1-piperazineethanesulfonic acid (HEPES), and BSA were purchased from Sigma Aldrich (St Louis, MO). Unfiltered human serum (hereafter, just "serum") was purchased from Millipore-Sigma (Taunton, MA). In some cases, the human serum was filtered using 10 kDa molecular weight cut-off spin filters (also from Millipore-Sigma), and this is hereafter referred to as "filtered serum". The 5 kDa methoxy poly(ethyleneglycol)thiol (mPEG-SH) was obtained from Nanocs (New York, NY).

Conductive carbon paste (Cl-2042) was purchased from Engineered Conductive Materials (Delaware, OH). Streptavidin-coated, 1.0 μm diameter magnetic beads (MμBs, Dynabeads, MyOne Streptavidin T1, 10 mg/mL) were obtained from Invitrogen (Grand Island, NY). Stock citrate-capped AgNPs (nominal 20 nm diameter, 0.18 mM Ag, 4.5×10^{11} NP/mL) were purchased from nanoComposix (San Diego, CA). N-terminal prohormone brain natriuretic peptide (NT-proBNP), monoclonal immunoglobulin G anti-NT-proBNP 13G12 detection (Ab), and 15C4 capture Ab were obtained from HyTest (Turku, Finland). The biotinylated polyclonal antimouse immunoglobulin G secondary antibody (SAb) was obtained from Abcam (Cambridge, UK). All solutions were made using deionized (DI) water (>18.0 MΩ cm, Milli-Q Gradient System, Millipore, Burlington, MA). All PBS concentrations were 1× unless otherwise noted.

Instrumentation. The UV−vis spectroscopic measurements were performed using a Hewlett-Packard HP8453 spectrometer with a 1.00 cm pathlength, micro-quartz cuvette (50 μL, Hellma, Müllheim, Germany). A tube revolver (cat. no. 88881001, Thermo Scientific) and a BioShake iQ from Quantifoil Instruments GmbH (Jena, Germany) were used for incubation steps during bioconjugation. Neodymium magnets were purchased from K&J Magnetics (Pipersville, PA) and were used for washing and separating steps involving magnetic microbeads (MμBs).

Electrochemistry. Electrochemical measurements were performed using a CH Instruments model 760B electrochemical workstation (Austin, TX). The fabrication of paper electrodes and electrodeposition of Au onto the WE are described in the Supporting Information and are based on a previous publication.[33] A previously published electrochemical protocol was used to detect the AgNP labels.[25,30,32,33] Briefly, to initiate GE, the potential of the WE was stepped from 0 to 0.80 V for 12.0 s to oxidize Au^0 to Au^{3+}. Following GE, the potential was stepped from 0 to −0.70 V for 50 s to electrodeposit Ag^0 onto the electrode. These two steps were carried out twice, and then, the potential was swept twice from −0.70 to 0.20 V at a scan rate of 50.0 mV/s to oxidize Ag^0. The charge resulting from the second linear-sweep ASV scan was obtained by integration of the area under the peak and represents the output signal of the sensor. Previous results from our group have shown that the area under the second ASV results in the largest and most reproducible charge signal.[32] All electrochemical measurements were performed in 1× PBS, unless stated otherwise, and all potentials are reported versus a carbon quasi-reference electrode (CQRE).

Preparation of Assay Components. 13G12 Ab was conjugated to the AgNPs using a previously published protocol[26] that is also discussed in more detail in the Supporting Information. Briefly, 13G12 Ab was modified by bioconjugation to a heterobifunctional cross-linker. The modified Ab was then added to 500 μL of AgNPs (4.9×10^{11} AgNPs/mL) and incubated for 1 h, followed by backfilling with mPEG-SH for 20 min at 600 rpm at room temperature (RT, 22 ± 3 °C). Excess conjugation reagents were then removed by centrifugation for 30 min at 16,600g at 4 °C. The formed bioconjugate was washed three times by centrifugation and then redispersed in 500 μL of SBB. Henceforth, this will be referred to as the AgNP-Ab conjugate.

For the model assay, the biotinylated SAb was conjugated to streptavidin-coated MμBs using the protocol provided by the manufacturer.[39] Specifically, 100 μL of MμBs (~$7-10 \times 10^9$ MμBs/mL) was aliquoted and washed. Washing was performed by magnetic separation, wherein the MμBs were collected on the wall of the tube with a neodymium magnet, the supernatant was removed, and the conjugate was redispersed in PBS. This was done three times within a SBB-blocked microcentrifuge tube. Next, 40.0 μL of 6.67 μM SAb was added, and the resulting solution was incubated for 30 min at 40 rpm at RT using the tube revolver. Finally, the conjugated MμBs were washed by magnetic separation five times with 100 μL of PBS−BSA solution (1% w/v in PBS) and redispersed in a final volume of 100 μL of the PBS−BSA solution. The resulting product is referred to as MμB-SAb.

In the case of the antigen-specific assay components, the 15C4 capture Ab was biotinylated using a kit and the protocol provided by the manufacturer.[40] After biotinylating the 15C4 capture Ab, the modified Ab was then conjugated to the streptavidin-coated MμBs using the same procedure as described for MμB-SAb, wherein 40.0 μL of the 6.67 μM biotinylated 15C4 capture Ab was incubated with 100 μL of the streptavidin-coated MμBs for 30 min at 40 rpm at RT on the tube revolver. After incubation, the conjugate was washed by

https://doi.org/10.1021/acssensors.1c00446
ACS Sens. 2021, 6, 1956−1962

magnetic separation. The resulting product is referred to as MμB-15C4.

Formation of the Metalloimmunoassays. Following preparation of the assay components, two different metalloimmunoassays were prepared: the model assay and the antigen-specific assay. The model assay was formed by bioconjugating MμB-SAb and AgNP-Ab through the attached Abs in either undiluted normal serum or PBS. Specifically, 16.0 μL of the as-prepared MμB-SAb was added to 100 μL of AgNP-Ab having the desired concentration in an SBB-blocked microcentrifuge tube and then incubated for 1.0 h in the tube revolver at 30 rpm. The components were washed with the 0.1% (v/v) Tween-20 and PBS solution three times using magnetic separation, and then they were redispersed in 16.0 μL of PBS. This conjugate will be referred to henceforth as the MμB-AgNP model composite.

A step-wise conjugation approach was used for the antigen-specific assay. More specifically, this assay was formed in a SBB-blocked microcentrifuge tube as follows. First, 16.0 μL of the MμB-15C4 conjugate was placed in a tube along with 100 μL of a known concentration of NT-proBNP in undiluted normal serum or PBS. These components were incubated for 30 min at 30 rpm at RT. Next, the partially formed assay was washed three times by magnetic separation with 0.1% (v/v) Tween-20 and PBS solution to remove the unbound peptide. Finally, 100 μL of the AgNP-Ab conjugate (in serum) was added. This mixture was incubated for 30 min at 30 rpm and was then washed by magnetic separation. The fully formed antigen-specific assay was resuspended in a final volume of 16.0 μL of PBS.

For analysis, both the model and the antigen-specific assays were prepared in a similar way in that 2.0 μL aliquots of the desired assay were combined with 48 μL of PBS in a tube to yield a final sample volume of 50.0 μL. These diluted samples were then transferred to the paper-based electrode, the fully formed assays were focused onto the WE (~30.0 s) by the magnet, and the electrochemical procedure was performed as discussed earlier.

Assay Washing Procedures. Two washing procedures were used: (1) washing of the MμB-AgNP model composite and (2) washing following dispersion of the formed MμB-AgNP model composite in different percentages of serum prior to electrochemical detection. The latter washing protocol is described next.

After formation of the MμB-AgNP model composite, initial electrochemical measurements were performed by dispersing 2.0 μL of the MμB-AgNP composite into 48.0 μL of the diluted serum matrix to yield a final sample volume of 50.0 μL and a final AgNP concentration of 100 pM. The percentages of serum were 100.0, 50.0, 20.0, 10.0, 5.0, 2.0, 1.0, 0.50, and 0.25%, and these serum solutions were diluted with PBS. Aliquots of 50.0 μL of these solutions were transferred onto the paper electrode, and then, the GE/ASV detection process was carried out. The first GE/ASV assay was carried out directly on these samples with no washing steps.

Following the foregoing initial electrochemical detection experiments, identical experiments were undertaken after washing. For the first washing step, the MμB-AgNP model composites were separated from the serum samples mentioned in the previous paragraph using a magnet. Next, they were redispersed in 50.0 μL of PBS, and then, the electrochemical assay was carried out using this solution. The second and third washing steps were performed the same way.

Ag^+ Electrodeposition. To better understand the impact of serum on the GE/ASV detection process, we examined the Ag^+ electrodeposition step in the presence of serum or filtered serum. The filtered serum was prepared by centrifuging 500.0 μL of serum for 10 min at 10,000*g* using a 10 kDa molecular weight cut-off spin filter. The filtrate was collected and used without further treatment.

The three test solutions used in this experiment contained the following components: (1) 1.0 mM $AgNO_3$ + 0.10 M KNO_3 in DI water, (2) 1.0 mM $AgNO_3$ + 0.10 M KNO_3 in 20.0% serum diluted with DI water, and (3) 1.0 mM $AgNO_3$ + 0.10 M KNO_3 in 20.0% filtered serum diluted with DI water. The Ag^+ electrodeposition experiments were carried out as follows. First, 50.0 μL of the desired test solution was placed on the WE. Second, the WE potential was stepped from 0 to −0.70 V (vs CQRE) for 50 s to reduce Ag^+ onto the electrode surface. Third, the electrodeposited Ag^0 was anodically stripped from the electrode surface by carrying out two consecutive, linear-potential scans from −0.70 to 0.20 V at a scan rate of 50 mV/s. The ASV data obtained from the second scan were collected and used for quantification.[32]

GE in Bulk Solution. GE of AgNPs by $HAuCl_4$ in bulk solution (no electrode) was studied by UV−vis spectroscopy. Before performing these experiments, the AgNPs were capped with mPEG-SH (hereafter referred to as Ag-mPEG) to yield AgNPs similar to those in the MμB-AgNP composite. The experiments were carried out by combining DI water, Ag-mPEG, $HAuCl_4$, and either serum or filtered serum in a 1.5 mL microcentrifuge tube. The resulting solutions were then mixed using a vortexer for ~30 s. The total volume for the solutions was 100.0 μL. The specific reagent usages for each experiment are provided in Table S1. A series of experiments was performed in which the percentage of serum or filtered serum was varied in the presence of a constant charge equivalent ratio of $HAuCl_4$ to Ag (because we do not necessarily know the speciation of oxidized Au in solution, we hereafter refer to all forms of oxidized Au as Au^{3+}). In all cases, the extent of GE was determined by transferring a portion of each sample to a 50.0 μL cuvette having a 1.00 cm pathlength and then analyzing the solutions by UV−vis spectroscopy.

RESULTS AND DISCUSSION

Effect of Serum on Assay Formation. A key step in biosensing is the formation of the assay, or, in other words, capture of the target molecule. Depending on the complexity of the matrix and the specificity of the capture molecules, this step can be challenging. Here, two different assays, the MμB-AgNP model composite and the antigen-specific assay for NT-proBNP, were prepared in different matrixes, and then, they were analyzed electrochemically. Each of the assays was formed in either PBS or serum. For all experiments in this section, the MμB-AgNP model composite contained 200 pM of AgNPs. The antigen-specific assay was prepared using a step-wise approach with 2.0 nM of NT-proBNP. Following formation of the assays, they were washed three times as described in the Experimental Section, transferred to the paper electrode, and analyzed by GE/ASV.

Figure 1a is a histogram showing the results of the foregoing experiment for the MμB-AgNP model composite. The results clearly indicate that, within experimental error, the total charge collected for the MμB-AgNP model composite is independent of whether the assay is formed in serum or PBS. An identical conclusion is obtained for the antigen-specific assay (Figure

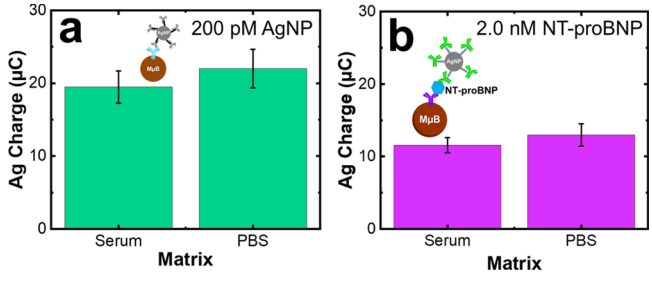

Figure 1. Histograms representing the Ag charge obtained when the (a) MμB-AgNP model composite (prepared using 200 pM AgNP) and (b) antigen-specific assay for NT-proBNP (prepared using 2.0 nM NT-proBNP) were formed in either PBS or serum. Following assay formation, the samples were both washed by magnetic separation and aliquoted, as described in the Experimental Section, and transferred to the paper electrode for analysis in 50.0 μL of PBS. The error bars represent the standard deviation from the mean for five independent measurements.

https://doi.org/10.1021/acssensors.1c00446
ACS Sens. 2021, 6, 1956−1962

1b). We conclude that the matrix in which the assay is formed does not impact the outcome of the GE/ASV detection method. To be clear, however, while the assays were formed in either serum or PBS, the actual electrochemical detection was carried out in aqueous PBS following washing of the assays with the 0.1% (v/v) Tween-20 and PBS.

Effect of Serum on Electrochemical Detection. After confirming that the serum matrix has no detectable impact on the formation of the two metalloimmunoassays, the impact of serum on electrochemical detection was studied. In this experiment, the MμB-AgNP model composite was prepared in PBS and then exposed to different percentages of diluted serum for 1−2 min. For all experiments in this section, the concentration of AgNPs was 100 pM. The preformed assays were then washed up to three times with PBS prior to analysis, and the resulting charge was determined using the GE/ASV method described earlier.

Figure 2 presents histograms showing the total charge recovered from the analysis of the MμB-AgNP model composite as a function of the number of washing steps and the percentage of serum. The black histograms correspond to the charge detected from the as-prepared model composite (no washing steps after exposure to the indicated percentages of serum). At serum percentages >5.0%, no Ag charge is detected, but for lower percentages, there is a gradual increase. For the smallest percentage of serum, 0.25%, a limiting charge of 10.6 ± 1.2 μC was detected. In other words, with no washing steps included in the protocol, the presence of even 0.50% serum renders the assay inaccurate.

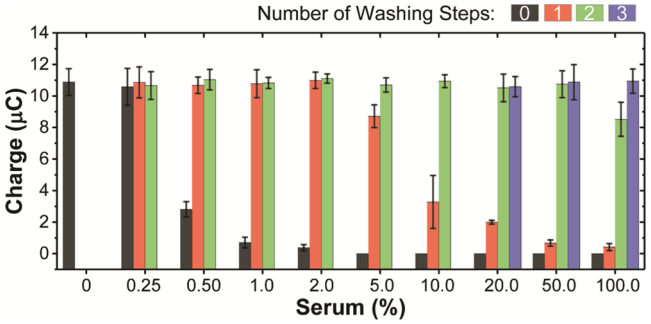

Figure 2. Histograms representing the amount of the Ag charge collected from the preformed MμB-AgNP model composite after it was exposed to various percentages of serum for 1−2 min and washed 0−3 times via magnetic separation. After washing, the samples were transferred to the paper electrode and the GE/ASV detection protocol was carried out using 50.0 μL of PBS. The error bars represent the standard deviation from the mean for three independent measurements.

The remaining histograms represent the charge recovered after the MμB-AgNP model composite was washed once, twice, or three times with PBS to remove residual serum prior to the electrochemical analysis. Specifically, after exposure to serum, 50.0 μL of the MμB-AgNP model composite was washed using magnetic separation and then redispersed in 50.0 μL PBS before electrochemical detection. The trends in Figure 2 are quite clear: lower percentages of serum require less washing steps to achieve limiting charge detection and more washing steps result in detection of higher charge. In fact, three washing steps result in limiting charge detection even after the model composite is exposed to 100% serum. This same experiment was performed with two other washing buffers (1× PBS + 1.0% Tween-20 and HEPES), and in both cases, the charge collected was lower than with 1× PBS only (Figure S1).

On the basis of the foregoing results, we conclude that even after exposure to relatively small amounts of serum, limiting charge detection cannot be obtained in the absence of washing. The question then remains: what exactly is the effect of serum on the GE/ASV electrochemical detection method and, by extension, other electrochemical detection methods?

Effect of Serum on Ag^+ Electrodeposition. Inhibition of electron and mass transfer by biofilms is a common problem in biosensing applications,[41,42] although there are some notable exceptions.[43−46] Accordingly, we evaluated the effect of serum on the GE/ASV detection method by isolating the electrodeposition step. This was achieved by eliminating the analyte and AgNPs from the assay and simply carrying out Ag^+ electrodeposition in solutions containing serum. Specifically, electrodeposition was performed in bulk solutions containing 1.0 mM of $AgNO_3$, 0.10 M KNO_3, and different percentages of serum. The electrochemistry itself was carried out by stepping the WE potential from 0 to −0.70 V for 50 s, and then, the potential was swept twice from −0.70 to 0.20 V. The second ASV was recorded, and the area under the peak was integrated to determine the charge.

Figure 3a shows three representative ASV traces collected using DI water, 20.0% serum, and 20.0% filtered serum.

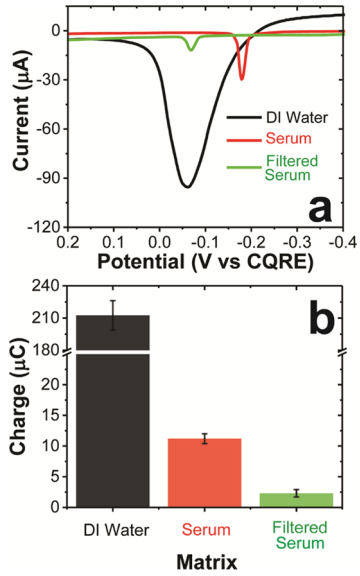

Figure 3. Effect of serum on Ag^+ electrodeposition. (a) ASVs obtained following electrodeposition of Ag^+ from 50.0 μL solutions (DI water, 20.0% serum, or 20.0% filtered serum) containing 1.0 mM $AgNO_3$ and 0.10 M KNO_3. Electrodeposition was carried out for 50 s at −0.70 V (vs CQRE) on the paper electrode platform. The ASV scan rate was 50 mV/s. (b) Histograms representing the amount of the Ag charge obtained by integrating the traces in (a). The error bars represent the standard deviation from the mean for three independent measurements.

Filtering removes components of the serum having molecular weights larger than about 10 kDa, principally, human serum albumin, globulin, and other large biomolecules. The important observation is that even the presence of 20.0% serum dramatically reduces the ASV charge. This finding is reinforced by the histograms shown in Figure 3b, which indicate a 20-fold decrease in charge for the serum solution. As

https://doi.org/10.1021/acssensors.1c00446
ACS Sens. 2021, 6, 1956−1962

an aside, it seems counterintuitive that filtered serum would have a more dramatic effect on ASV than the serum (Figure 3b), and except for pointing out that this observation is reproducible we are unable to offer an explanation for this finding.

We propose that the underlying reason for the dramatic effect of serum on Ag^+ electrodeposition may relate to either of the following two factors. First, it has previously been reported that Ag^+ is chelated by albumin, which is present in serum.[47] Therefore, the presence of albumin or other biomolecules in serum can cause chelation, which shifts the redox potential of ions to more negative potentials in proportion to the strength of binding.[2,48] A second possible effect of serum on electrodeposition relates to electrode passivation by biomolecules. Passivation can hinder electron transfer, mass transfer, or both (Figure S2).[49,50]

Impact of Serum on GE in Bulk Solution. Apart from the Ag^+ electrodeposition step, the other important reaction in the GE/ASV detection process is GE. Therefore, in this section, we examine the impact of serum on GE.

As shown in Scheme 1a, detection in the electrochemical assay is initiated by first generating Au^{3+} by electro-oxidation of metallic Au predeposited on the paper electrode. Because this step is necessary for GE, we investigated it in the presence of serum first. As shown in Figure S3, the result is that there is no statistically significant difference in the charge recorded for Au oxidation when using PBS or PBS plus 20.0% serum. Accordingly, we conclude that serum does not affect the first step of the GE process.

After determining that the Au^{3+} electrogeneration step is unhindered by serum, the GE reaction between Au^{3+} and Ag-mPEG was analyzed in bulk solution (Scheme 1a). Ag-mPEG was used as the model AgNP label because of its similarity to the Ag labels in the MμB-AgNP model composite. Recall that in this composite, the Ab-modified AgNPs are back-filled with mPEG-SH to improve NP stability. Accordingly, the only difference between Ag-mPEG and the AgNP-Ab bioconjugate is the presence of MμBs and Abs in the latter.

The GE experiments were performed by combining DI water; Ag-mPEG; Au^{3+}; and serum, or filtered serum in a microcentrifuge tube and vortexing for ~30 s. Following mixing, the solutions were analyzed by UV−vis spectroscopy. It should be noted that Au^{3+} was introduced into the system with increasing equivalents of charge. For example, one charge equivalent of Au^{3+} corresponds to 3.00 nmol Au atoms for every 9.00 nmol Ag atoms.

The black trace shown in Figure 4a is an absorbance spectrum of Ag-mPEG in DI water. It exhibits a surface plasmon resonance (SPR) peak at ~400 nm arising from the AgNPs. When one charge equivalent of Au^{3+} is introduced into this solution, the red trace results after just 1 min. The loss of the SPR peak indicates that Ag-mPEG was converted to Ag^+ via GE. One might expect the presence of a new AuNP SPR peak in the red spectrum following GE, and in fact, a peak at 535 nm does emerge after 4 h (Figure S4).

When the foregoing experiment is carried out in a matrix containing 20.0% serum instead of DI water (Figure 4b), there is no change in the absorbance of the SPR peak following the addition of Au^{3+}. This finding indicates that even 20.0% serum completely inhibits GE. The results of additional experiments in which the percentage of serum was varied are presented in Figure S5. These spectra show that even 2.0% serum partially inhibits GE.

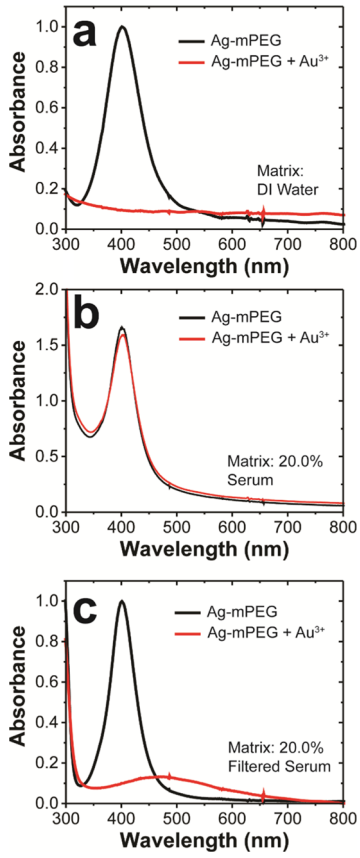

Figure 4. Representative UV−vis spectra of Ag-mPEG before (black trace) and after (red trace) the addition of about one charge equivalent of Au^{3+} relative to Ag in (a) DI water, (b) 20.0% serum, and (c) 20.0% filtered serum. The peak at ~400 nm is due to the SPR of AgNPs.

Interestingly, as shown in Figure 4c, when the serum was filtered through a 10 kDa molecular weight cut-off filter and used in place of water, the intensity of the peak decreased by 87%, indicating that the extent of GE is only slightly affected in this case. This indicates that biomolecules having molecular weights >10 kDa are principally responsible for inhibition of GE, but lower molecular weight molecules also contribute to inhibition. In addition to the decrease in the magnitude of the absorbance peak, the peak position shifts from ~400 to ~480 nm. This change suggests that the products of the GE may be different depending on whether the reaction is carried out in 20.0% filtered serum or DI water.[51]

Taking into account the foregoing discussion, we conclude there are two possible explanations for the inhibition of GE by serum. First, biomolecules may adsorb to the surface of the Ag-mPEG NPs and prevent penetration by Au^{3+}, thereby inhibiting GE by limiting mass transfer. The second possibility is that biomolecules present in serum chelate Au^{3+}, which would shift its redox potential into a regime that hinders GE.[2,48] At present, we are unable to determine if one or both of these mechanisms is responsible for suppression of GE.

SUMMARY AND CONCLUSIONS

To summarize, the goal of this study was to determine the effect of serum on electrochemical bioassays that use AgNPs as detection labels. Using a GE/ASV detection method previously developed in our group,[32] we confirmed that both a model and

https://doi.org/10.1021/acssensors.1c00446
ACS Sens. 2021, 6, 1956−1962

an antigen-specific assay for NT-proBNP could be formed in undiluted serum with no detectable adverse effects from the matrix. In addition to assay formation, we also performed a systematic analysis of the washing steps. This part of the study revealed that there is a high degree of signal inhibition in the absence of washing if even 0.50% of serum remains in solution.

Inhibition of electron and mass transfer by biofilms is a common issue in biosensing applications, and therefore, this study offers generally useful insights into how this problem affects electrochemical detection of NP labels. Accordingly, the results are likely to be valuable to many in the field of chemical sensing. The findings described here will be applied to the ongoing development of a biosensor for heart failure that is currently underway in our lab. The results of that work will be reported in due course.

■ ASSOCIATED CONTENT

Supporting Information

The Supporting Information is available free of charge at https://pubs.acs.org/doi/10.1021/acssensors.1c00446.

Procedure for the fabrication of the paper electrodes; reagents used for GE in different percentages of serum, filtered serum, and DI water; effect of different buffers on serum washing steps; effect of serum on mass transfer and electron transfer; effect of serum on the electro-oxidation of Au; UV−vis spectra of Ag-mPEG before and after GE for 1 min and 4 h in DI water; and UV−vis spectra of Ag-mPEG before and after GE in serum (PDF)

■ AUTHOR INFORMATION

Corresponding Author

Richard M. Crooks − *Department of Chemistry, The University of Texas at Austin, Austin, Texas 78712-1224, United States;* orcid.org/0000-0001-5186-4878; Email: crooks@cm.utexas.edu

Authors

Nicole E. Pollok − *Department of Chemistry, The University of Texas at Austin, Austin, Texas 78712-1224, United States*

Yi Peng − *Department of Chemistry, The University of Texas at Austin, Austin, Texas 78712-1224, United States;* orcid.org/0000-0002-5319-1336

Charlie Rabin − *Department of Chemistry, The University of Texas at Austin, Austin, Texas 78712-1224, United States*

Ian Richards − *Interactives Executive Excellence LLC, Austin, Texas 78733, United States*

Complete contact information is available at: https://pubs.acs.org/10.1021/acssensors.1c00446

Author Contributions

§N.E.P. and Y.P. contributed equally.

Notes

The authors declare the following competing financial interest(s): Richard Crooks and Ian Richards are associated with Galvanyx, LLC, and the research reported herein could be useful to this entity in the future.

■ ACKNOWLEDGMENTS

Research reported in this publication was supported by the National Heart, Lung, and Blood Institute of the National Institutes of Health under Award R01HL137601. The content is solely the responsibility of the authors and does not necessarily represent the official views of the National Institutes of Health. We also thank the Robert A. Welch Foundation (grant F-0032) for sustained support of our research.

■ REFERENCES

(1) Matei, I.; Buta, C. M.; Turcu, I. M.; Culita, D.; Munteanu, C.; Ionita, G. Formation and Stabilization of Gold Nanoparticles in Bovine Serum Albumin Solution. *Molecules* **2019**, *24*, 3395.

(2) Gebregeorgis, A.; Bhan, C.; Wilson, O.; Raghavan, D. Characterization of Silver/Bovine Serum Albumin (Ag/BSA) Nanoparticles Structure: Morphological, Compositional, and Interaction Studies. *J. Colloid Interface Sci.* **2013**, *389*, 31−41.

(3) Stankovich, M. T.; Bard, A. J. The Electrochemistry of Proteins and Related Substances Part III. Bovine Serum Albumin. *J. Electroanal. Chem.* **1978**, *86*, 189−199.

(4) You, M.; Lin, M.; Gong, Y.; Wang, S.; Li, A.; Ji, L.; Zhao, H.; Ling, K.; Wen, T.; Huang, Y.; et al. Household Fluorescent Lateral Flow Strip Platform for Sensitive and Quantitative Prognosis of Heart Failure Using Dual-Color Upconversion Nanoparticles. *ACS Nano* **2017**, *11*, 6261−6270.

(5) Heller, A.; Feldman, B. Electrochemical Glucose Sensors and Their Applications in Diabetes Management. *Chem. Rev.* **2008**, *108*, 2482−2505.

(6) Ng, V. L.; Kraemer, R.; Hogan, C.; Eckman, D.; Siobal, M. The Rise and Fall of I-STAT Point-of-Care Blood Gas Testing in an Acute Care Hospital. *Am. J. Clin. Pathol.* **2000**, *114*, 128−138.

(7) Malhotra, B. D.; Chaubey, A. Biosensors for Clinical Diagnostics Industry. *Sens. Actuators, B* **2003**, *91*, 117−127.

(8) Erickson, K. A.; Wilding, P. Evaluation of a Novel Point-of-Care System, the i-STAT Portable Clinical Analyzer. *Clin. Chem.* **1993**, *39*, 283−287.

(9) Sarangadharan, I.; Wang, S.-L.; Sukesan, R.; Chen, P.-c.; Dai, T.-Y.; Pulikkathodi, A. K.; Hsu, C.-P.; Chiang, H.-H. K.; Liu, L. Y.-M.; Wang, Y.-L. Single Drop Whole Blood Diagnostics: Portable Biomedical Sensor for Cardiac Troponin I Detection. *Anal. Chem.* **2018**, *90*, 2867−2874.

(10) Sinawang, P. D.; Harpaz, D.; Fajs, L.; Seet, R. C. S.; Tok, A. I. Y.; Marks, R. S. Electrochemical Impedimetric Detection of Stroke Biomarker NT-ProBNP Using Disposable Screen-Printed Gold Electrodes. *EuroBiotech J.* **2017**, *1*, 165−176.

(11) Song, Y.; Min, J.; Yu, Y.; Wang, H.; Yang, Y.; Zhang, H.; Gao, W. Wireless Battery-Free Wearable Sweat Sensor Powered by Human Motion. *Sci. Adv.* **2020**, *6*, No. eaay9842.

(12) Wang, Z.; Gui, M.; Asif, M.; Yu, Y.; Dong, S.; Wang, H.; Wang, W.; Wang, F.; Xiao, F.; Liu, H. A Facile Modular Approach to the 2D Oriented Assembly MOF Electrode for Non-Enzymatic Sweat Biosensors. *Nanoscale* **2018**, *10*, 6629−6638.

(13) Oncescu, V.; O'Dell, D.; Erickson, D. Smartphone Based Health Accessory for Colorimetric Detection of Biomarkers in Sweat and Saliva. *Lab Chip* **2013**, *13*, 3232−3238.

(14) Rehman, S. A.; Khurshid, Z.; Niazi, F. H.; Naseem, M.; Waddani, H. Al; Sahibzada, H. A.; Khan, R. S. Role of Salivary Biomarkers in Detection of Cardiovascular Diseases (CVD). *Proteomes* **2017**, *5*, 21.

(15) Chekin, F.; Vasilescu, A.; Jijie, R.; Singh, S. K.; Kurungot, S.; Iancu, M.; Badea, G.; Boukherroub, R.; Szunerits, S. Sensitive Electrochemical Detection of Cardiac Troponin I in Serum and Saliva by Nitrogen-Doped Porous Reduced Graphene Oxide Electrode. *Sens. Actuators, B* **2018**, *262*, 180−187.

(16) Deng, M.; Li, M.; Li, F.; Mao, X.; Li, Q.; Shen, J.; Fan, C.; Zuo, X. Programming Accessibility of DNA Monolayers for Degradation-Free Whole-Blood Biosensors. *ACS Mater. Lett.* **2019**, *1*, 671−676.

(17) Magner, E. Detection of Ferricyanide as a Probe for the Effect of Hematocrit in Whole Blood Biosensors. *Analyst* **2001**, *126*, 861−865.

(18) Wu, J.; Dong, M.; Zhang, C.; Wang, Y.; Xie, M.; Chen, Y. Magnetic Lateral Flow Strip for the Detection of Cocaine in Urine by Naked Eyes and Smart Phone Camera. *Sensors* **2017**, *17*, 1286.
(19) Krebs, H. A. Chemical Composition of Blood Plasma and Serum. *Annu. Rev. Biochem.* **1950**, *19*, 409−430.
(20) Havel, R. J.; Eder, H. A.; Bragdon, J. H. The Distribution and Chemical Composition of Ultracentrifugally Separated Lipoproteins in Human Serum. *J. Clin. Invest.* **1955**, *34*, 1345−1353.
(21) Mohammed, M.-I.; Desmulliez, M. P. Y. Lab-on-a-Chip Based Immunosensor Principles and Technologies for the Detection of Cardiac Biomarkers: A Review. *Lab Chip* **2011**, *11*, 569−595.
(22) Mainville, C. A.; Clark, G. H.; Esty, K. J.; Foster, W. M.; Hanscom, J. L.; Hebert, K. J.; Lyons, H. R. Analytical Validation of an Immunoassay for the Quantification of N-Terminal pro−B-Type Natriuretic Peptide in Feline Blood. *J. Vet. Diagn. Invest.* **2015**, *27*, 414−421.
(23) Labib, M.; Sargent, E. H.; Kelley, S. O. Electrochemical Methods for the Analysis of Clinically Relevant Biomolecules. *Chem. Rev.* **2016**, *116*, 9001−9090.
(24) Dequaire, M.; Degrand, C.; Limoges, B. An Electrochemical Metalloimmunoassay Based on a Colloidal Gold Label. *Anal. Chem.* **2000**, *72*, 5521−5528.
(25) Pollok, N. E.; Rabin, C.; Walgama, C. T.; Smith, L.; Richards, I.; Crooks, R. M. Electrochemical Detection of NT-ProBNP Using a Metalloimmunoassay on a Paper Electrode Platform. *ACS Sens.* **2020**, *5*, 853−860.
(26) Pollok, N. E.; Rabin, C.; Smith, L.; Crooks, R. M. Orientation-Controlled Bioconjugation of Antibodies to Silver Nanoparticles. *Bioconjugate Chem.* **2019**, *30*, 3078−3086.
(27) Conroy, P. J.; Hearty, S.; Leonard, P.; O'Kennedy, R. J. Antibody Production, Design and Use for Biosensor-Based Applications. *Semin. Cell Dev. Biol.* **2009**, *20*, 10−26.
(28) DeGregory, P. R.; Tsai, Y.-J.; Scida, K.; Richards, I.; Crooks, R. M. Quantitative Electrochemical Metalloimmunoassay for TFF3 in Urine Using a Paper Analytical Device. *Analyst* **2016**, *141*, 1734−1744.
(29) Zhang, L.; Hu, D.; Salmain, M.; Liedberg, B.; Boujday, S. Direct Quantification of Surface Coverage of Antibody in IgG-Gold Nanoparticles Conjugates. *Talanta* **2019**, *204*, 875−881.
(30) DeGregory, P. R.; Tapia, J.; Wong, T.; Villa, J.; Richards, I.; Crooks, R. M. Managing Heart Failure at Home with Point-of-Care Diagnostics. *IEEE J. Transl. Eng. Health Med.* **2017**, *5*, 2800206.
(31) Li, X.; Scida, K.; Crooks, R. M. Detection of Hepatitis B Virus DNA with a Paper Electrochemical Sensor. *Anal. Chem.* **2015**, *87*, 9009−9015.
(32) Cunningham, J. C.; Kogan, M. R.; Tsai, Y.-J.; Luo, L.; Richards, I.; Crooks, R. M. Paper-Based Sensor for Electrochemical Detection of Silver Nanoparticle Labels by Galvanic Exchange. *ACS Sens.* **2016**, *1*, 40−47.
(33) Kogan, M. R.; Pollok, N. E.; Crooks, R. M. Detection of Silver Nanoparticles by Electrochemically Activated Galvanic Exchange. *Langmuir* **2018**, *34*, 15719−15726.
(34) Sinha, A.; Gopinnathan, P.; Chung, Y.-D.; Shiesh, S.-C.; Lee, G.-B. Simultaneous Detection of Multiple NT-ProBNP Clinical Samples Utilizing an Aptamer-Based Sandwich Assay on an Integrated Microfluidic System. *Lab Chip* **2019**, *19*, 1676−1685.
(35) Liu, C.; Leng, W.; Vikesland, P. J. Controlled Evaluation of the Impacts of Surface Coatings on Silver Nanoparticle Dissolution Rates. *Environ. Sci. Technol.* **2018**, *52*, 2726−2734.
(36) Hernández-Santos, D.; González-García, M. B.; García, A. C. Metal-Nanoparticles Based Electroanalysis. *Electroanalysis* **2002**, *14*, 1225−1235.
(37) Binaymotlagh, R.; Hadadzadeh, H.; Farrokhpour, H.; Haghighi, F. H.; Abyar, F.; Mirahmadi-Zare, S. Z. In Situ Generation of the Gold Nanoparticles-Bovine Serum Albumin (AuNPs-BSA) Bioconjugated System Using Pulsed-Laser Ablation (PLA). *Mater. Chem. Phys.* **2016**, *177*, 360−370.
(38) Murawala, P.; Phadnis, S. M.; Bhonde, R. R.; Prasad, B. L. V. In Situ Synthesis of Water Dispersible Bovine Serum Albumin Capped Gold and Silver Nanoparticles and Their Cytocompatibility Studies. *Colloids Surf., B* **2009**, *73*, 224−228.
(39) Thermo Fisher. *Dynabeads MyOne Streptavidin T1 Protocol*, 2016.
(40) Bio-Rad Laboratories. *LYNX Rapid Plus Biotin (Type 2) Antibody Conjugation Kit Protocol*, 2011, 2−4.
(41) Raditya, A. N.; O'Hare, D. Review-Electrochemical Sensor Biofouling in Environmental Sensor Networks: Characterisation, Remediation and Lessons from Biomedical Devices. *J. Electrochem. Soc.* **2020**, *167*, 127503.
(42) Wisniewski, N.; Reichert, M. Methods for Reducing Biosensor Membrane Biofouling. *Colloids Surf., B* **2000**, *18*, 197−219.
(43) Das, J.; Kelley, S. O. Protein Detection Using Arrayed Microsensor Chips: Tuning Sensor Footprint to Achieve Ultrasensitive Readout of CA-125 in Serum and Whole Blood. *Anal. Chem.* **2011**, *83*, 1167−1172.
(44) Álvarez-Martos, I.; Møller, A.; Ferapontova, E. E. Dopamine Binding and Analysis in Undiluted Human Serum and Blood by the RNA-Aptamer Electrode. *ACS Chem. Neurosci.* **2019**, *10*, 1706−1715.
(45) Nemr, C. R.; Smith, S. J.; Liu, W.; Mepham, A. H.; Mohamadi, R. M.; Labib, M.; Kelley, S. O. Nanoparticle-Mediated Capture and Electrochemical Detection of Methicillin-Resistant Staphylococcus Aureus. *Anal. Chem.* **2019**, *91*, 2847−2853.
(46) Rowe, A. A.; Chuh, K. N.; Lubin, A. A.; Miller, E. A.; Cook, B.; Hollis, D.; Plaxco, K. W. Electrochemical Biosensors Employing an Internal Electrode Attachment Site and Achieving Reversible, High Gain Detection of Specific Nucleic Acid Sequences. *Anal. Chem.* **2011**, *83*, 9462−9466.
(47) Ostermeyer, A.-K.; Kostigen Mumuper, C.; Semprini, L.; Radniecki, T. Influence of Bovine Serum Albumin and Alginate on Silver Nanoparticle Dissolution and Toxicity to Nitrosomonas Europaea. *Environ. Sci. Technol.* **2013**, *47*, 14403−14410.
(48) Bard, A. J.; Faulkner, L. R. *Electrochemical Methods: Fundamentals and Applications*; Harris, D.; Swain, E.; Robey, C.; Aiello, E., Eds.; 2nd ed.; John Wiley & Sons, Inc.: Hoboken, 2001.
(49) Chen, P.; McCreery, R. L. Control of Electron Transfer Kinetics at Glassy Carbon Electrodes by Specific Surface Modification. *Anal. Chem.* **1996**, *68*, 3958−3965.
(50) Doneux, T.; De Ghellinck, A.; Triffaux, E.; Brouette, N.; Sferrazza, M.; Buess-Herman, C. Electron Transfer Across an Antifouling Mercapto-Hepta(Ethylene Glycol) Self-Assembled Monolayer. *J. Phys. Chem. C* **2016**, *120*, 15915−15922.
(51) Monga, A.; Pal, B. Morphological and Physicochemical Properties of Ag-Au Binary Nanocomposites Prepared Using Different Surfactant Capped Ag Nanoparticles. *RSC Adv.* **2015**, *5*, 39954−39963.

https://doi.org/10.1021/acssensors.1c00446
ACS Sens. 2021, 6, 1956−1962